JOURNAL OF VIROLOGY, May 1997, p. 3726–3733 Vol. 71, No. 5
0022-538X/97/$04.00+0


# The Geminivirus BL1 Movement Protein Is Associated with Endoplasmic Reticulum-Derived Tubules in Developing Phloem Cells

BRIAN M. WARD,[1] RICHARD MEDVILLE,[2] SONDRA G. LAZAROWITZ,[1]* AND ROBERT TURGEON[3]

*Department of Microbiology, University of Illinois at Urbana-Champaign, Urbana, Illinois 61801,[1] and Electron Microscopy Services[2] and Section of Plant Biology, Division of Biological Sciences, Cornell University,[3] Ithaca, New York 14853*

Received 19 August 1996/Accepted 15 January 1997

**Plant viruses encode movement proteins that are essential for systemic infection of their host but dispensable for replication and encapsidation. BL1, one of the two movement proteins encoded by the bipartite geminivirus squash leaf curl virus, was immunolocalized to unique ~40-nm tubules that extended up to and across the walls of procambial cells in systemically infected pumpkin leaves. These tubules were not found in procambial cells from pumpkin seedlings inoculated with BL1 mutants that are defective in movement. The tubules also specifically stained with antisera to binding protein (BiP), indicating that they were derived from the endoplasmic reticulum. Independent confirmation of this endoplasmic reticulum association was obtained by subcellular fractionation studies in which BL1 was localized to fractions that contained both endoplasmic reticulum membranes and BiP. Thus, squash leaf curl virus appears to recruit the endoplasmic reticulum as a conduit for cell-to-cell movement of the viral genome.**

The pathogenic effects of plant viruses are due not to local infections but to systemic spread in which the virus moves locally from cell to cell and travels to distant parts of the plant via the phloem (2, 21). Resistance to plant viruses, whether naturally occurring or genetically engineered, often takes the form of resistance to movement (2, 21, 27, 35). Two types of cell-to-cell movement have been documented, both mediated by virus-encoded movement proteins (10, 12, 17, 34). In the first, typified by tobacco mosaic virus (TMV) and red clover necrotic mosaic virus, the movement protein (MP) functions as a molecular chaperone that binds the viral RNA genome and targets it to plasmodesmata, where the MP then appears to increase the size exclusion limits and move the viral genome through these intercellular channels without visibly altering their structure (8, 9, 15, 60, 63). In the second type of movement, employed by the comoviruses (57), nepoviruses (61), tospoviruses (24), and caulimoviruses (32), the MP has been immunolocalized to unique tubular structures that extend from the cell walls of mesophyll cells and have virus-like particles associated with or within them. When transiently expressed in protoplasts, the MP of these viruses (44, 51, 56) is sufficient to induce these tubular structures. In addition, mutational studies of cowpea mosaic virus (CPMV) demonstrate that viral coat protein is needed to form the virus-like particles within the tubules but not the tubules themselves (62). Thus, for these viruses it is proposed that virus-like particles, which appear to be virions or subviral particles, pass from one cell to another via tubules that are at least in part composed of the MP. These tubules are often reported to extend from plasmodesmata, although structural features typical of plasmodesmata, such as the desmotubule, are not seen at the regions where these tubules intersect the cell wall.

Geminiviruses are the only major group of plant viruses that possess single-stranded DNA (ssDNA) genomes (29, 50). Squash leaf curl virus (SqLCV) is phloem limited and, like all bipartite geminiviruses, encodes two proteins required for virus movement, BR1 and BL1 (22). Recent biochemical, molecular, and cellular studies have defined several functions of BR1 and BL1 in viral genome movement. BR1 is an ssDNA binding protein that localizes to nuclei of infected cells and functions as a nuclear shuttle protein (42, 47). BL1 is directly responsible for viral pathogenic properties (41), and transient expression assays in tobacco protoplasts demonstrate that BL1 provides directionality to viral movement by cooperatively interacting with BR1 to redirect it from the nucleus to the cell periphery (48, 49). Based on these results, we have proposed that BR1 binds the viral ssDNA genome, shuttling it between the nucleus and cytoplasm, where BL1 traps these BR1-ssDNA complexes and then acts to guide them to adjacent uninfected cells. In contrast, Noueiry et al. (38) postulated, based exclusively on microinjection experiments, that BL1 directly potentiates the movement of viral double-stranded DNA through plasmodesmata in much the same way reported for the function of the TMV MP in moving RNA. Clearly, precise information about the subcellular location of BL1 in infected plants is required to gain a better understanding of the role of BL1 in facilitating virus movement.

To further investigate the function of BL1, we have examined systemically infected pumpkin leaf tissue in which the invading SqLCV was moving along its natural route. In the undifferentiated phloem of the minor veins of these leaves, we observed unique tubules that were not seen in uninfected plants or in plants inoculated with SqLCV BL1 mutants that are defective in movement. Immunogold labeling showed BL1 to be specifically associated with these tubules and, combined with subcellular fractionation studies, suggested that the tubules were derived from the endoplasmic reticulum (ER). These results suggest that SqLCV BL1 interacts with the ER to form channels for the intercellular movement of BR1-genome complexes and that this interaction may be developmentally regulated.

* Corresponding author. Phone: (217) 333-0390. Fax: (217) 244-6697. E-mail: sondrala@uiuc.edu.

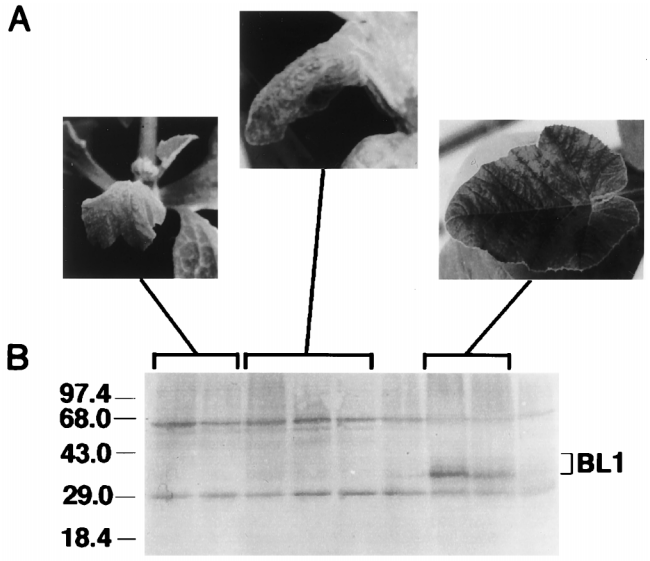


FIG. 1. (A) Left, leaf showing drooping at the margins of the lamina; middle, leaf at late stage of symptom development, showing chlorosis and severe epinasty; right, leaf at earliest stages of symptom development, showing mild chlorosis and no epinasty. (B) Immunoblot of BL1 extracted from systemic pumpkin leaves at different stages in symptom development, as indicated. Sizes are indicated in kilodaltons.

## MATERIALS AND METHODS

**Growth and agroinoculation of pumpkin seedlings with SqLCV.** Pumpkin (*Cucurbita maxima* L. cv. Big Max) was grown and maintained in peat-soil-perlite (1:1:1), either in a growth chamber or in a greenhouse with 16-h light cycles at 26°C/22°C daytime/nighttime temperatures. Cotyledons of 6-day-old pumpkin seedlings were agroinoculated with SqLCV-E DNA as previously described (30, 31).

**Subcellular fractionation and Western blotting.** To examine the levels of BL1 expression at different stages of symptom development, systemic leaves exhibiting a range of symptoms from mildly chlorotic to extremely chlorotic and epinastic were harvested at 6 to 8 days postinoculation. These were ground to a fine powder under liquid nitrogen and resuspended in 2.5 ml of grinding buffer (100 mM Tris–10 mM EDTA [pH 8.0], 5 mM dithiothreitol [DTT], 1 mM phenylmethylsulfonyl fluoride) per g of tissue. Sodium dodecyl sulfate was added to a final concentration of 3%, and samples were boiled for 5 min. Equal volumes of each extract were analyzed by sodium dodecyl sulfate-polyacrylamide gel electrophoresis on 12% polyacrylamide gels, using the discontinuous buffer system (26). Resolved proteins were immunoblotted as previously described (41).

For the separation of subcellular fractions by differential centrifugation, leaves displaying early disease symptoms of mild chlorosis without visible leaf curl (Fig. 1A, right) were cut into small pieces with a razor blade, placed in chilled tissue fractionation buffer (TFB; 10 ml/g; 400 mM sucrose, 50 mM HEPES, 10 mM KCl, 3 mM EGTA, 3 mM DTT, 1% bovine serum albumin, 1 mM phenylmethylsulfonyl fluoride, adjusted to pH 7.6 with bis-Tris propane), and vacuum infiltrated three times for 2 min each. All subsequent steps were done at 4°C. Tissue was homogenized for 3 min in a Polytron PT 3000 (Brinkmann) set at 3,000 rpm, and the homogenate was filtered through one layer of Miracloth (Calbiochem) and centrifuged at $1{,}000 \times g_{av}$ for 15 min to obtain an S1 supernatant and P1 pellet (crude cell wall fraction [41]). The supernatant (S1) was removed and centrifuged at $5{,}200 \times g_{av}$ for 80 min to give a pellet (P2), which contained the Golgi and plasma membranes, and the supernatant (S2). ER membranes were pelleted from the S2 supernatant by centrifugation at $100{,}000 \times g_{av}$ for 1 h. Pelleted membranes were further separated by the aqueous two-phase partition method (28) as modified by Bush (6). Pellets recovered from each partitioned phase were resuspended in TFB (minus DTT and bovine serum albumin)–10% glycerol, and 100-μl aliquots were stored frozen at −80°C for enzyme assays and Western blot analyses.

Subcellular fractions containing ER, Golgi, or plasma membranes were identified by assaying for antimycin A-insensitive NADH-dependent cytochrome *c* reductase, Triton-stimulated IDPase, or vanadate-sensitive $K^+$-$Mg^{2+}$-ATPase, respectively, as described by Bush (6).

**Immunogold labeling of thin sections.** Tissue samples were fixed in 0.5% glutaraldehyde–3% paraformaldehyde in 50 mM piperazine-*N*,*N*′-bis(2-ethanesulfonic acid) (PIPES) buffer containing 2 mM $CaCl_2$ (pH 7.2) for 2.5 h at 4°C. Fixed samples were washed in the same buffer and dehydrated over a period of 1 h in a graded ethanol series to a final concentration of 90% ethanol. Temperature was progressively lowered during dehydration to −20°C at the 60% ethanol stage, and all subsequent embedding steps were carried out at −20°C. Samples were embedded in LR White resin (medium grade; Electron Microscopy Sciences) over a 3-day period and then placed in gelatin capsules and hardened at 52°C. Ultramicrotomy, immunocytochemical staining using specific antisera and protein A-colloidal gold, and electron microscopy were all performed as previously described (42, 55). Anti-BL1 antisera (41, 48) and anti-BiP antisera (64) were each used at a 1:500 dilution. Colloidal gold particles (20 nm) coupled to protein A were obtained from Electron Microscopy Sciences and used according to the manufacturer's recommendations.

**Source of antisera.** Rabbit polyclonal antisera against BL1 were generated against gel-purified BL1 that had been overexpressed in *Escherichia coli* and have been described elsewhere (41, 48). Affinity-purified rabbit polyclonal antisera against BiP purified from maize kernels (14) were a kind gift of Rebecca Boston.

## RESULTS

**Unique tubules are present in pumpkin leaves systemically infected with SqLCV.** Cotyledons of 6-day-old pumpkin seedlings (*C. maxima* L. cv. Big Max) were agroinoculated with SqLCV DNA (30). Six days postinoculation, the second true leaf (~4 cm in length) had unfolded from the apex and was just beginning to show the first signs of disease symptoms, a mild but distinct chlorosis (Fig. 1A, right) that always preceded drooping at the margins of the lamina and the final development of severe epinasty (downward leaf curl) in the expanded leaf (Fig. 1A, middle). BL1 accumulation was correlated with the stages of symptom development, with BL1 at maximal levels at the earliest stage of mild chlorosis preceding any evidence of epinasty (Fig. 1A, right). As the severity of symptoms progressed in individual systemic leaves, levels of BL1 decreased (Fig. 1A, left and middle). Thus, tissue samples from the median region of leaves at the earliest stage of disease development were excised, fixed, and embedded for immunocytochemistry or extracted for subcellular fractionation studies (see below).

At this stage of leaf development, mesophyll cells were densely cytoplasmic, there were no intercellular spaces, and the tissue was still a sink for photoassimilate; that is, it had not yet begun to export (53). The large veins had fully differentiated phloem and xylem, but the minor veins were completely undifferentiated. The division of meristematic cells to form separate companion cells and sieve elements in the minor vein phloem does not occur in the leaves of cucurbitaceous species until shortly before the sink-source transition (59). Therefore, mitotic divisions in the minor veins of these young leaves were not complete. Nonetheless, the procambial cells (undifferentiated vascular tissue) of which the veins are composed were easily recognized by their elongated shape and characteristic position in the middle layers of the lamina.

Unique tubules were seen in procambial cells of these systemically infected leaves (Fig. 2 to 4). These tubules were not seen in the developing mesophyll, nor were they found in procambial cells from uninfected plants. The tubules were also not seen in plants inoculated with BL1 missense mutants $BL1^{R96A}$ and $BL1^{W208A}$, both of which are defective for virus movement and null in infectivity (not shown) (48). Tubules were unbranched, relatively straight but sometimes curved, and usually oriented at right angles to the cell wall. The walls from which the tubules extended were typically quite thin, thus indicating that they were probably newly formed (Fig. 2, 3A, B, and D, and 4). In many cases, the tubules ended at the cell wall or slightly within it; however, in other instances these tubules clearly extended from one cell to another through the wall (Fig. 3A and B and 4). Where the tubules crossed the wall, there was no visible desmotubule or other structural features characteristic of plasmodesmata (Fig. 3A, B, and D and 4). Thus, if such an association existed, visible remnants of plasmodesmal structures within the wall must have been altered or

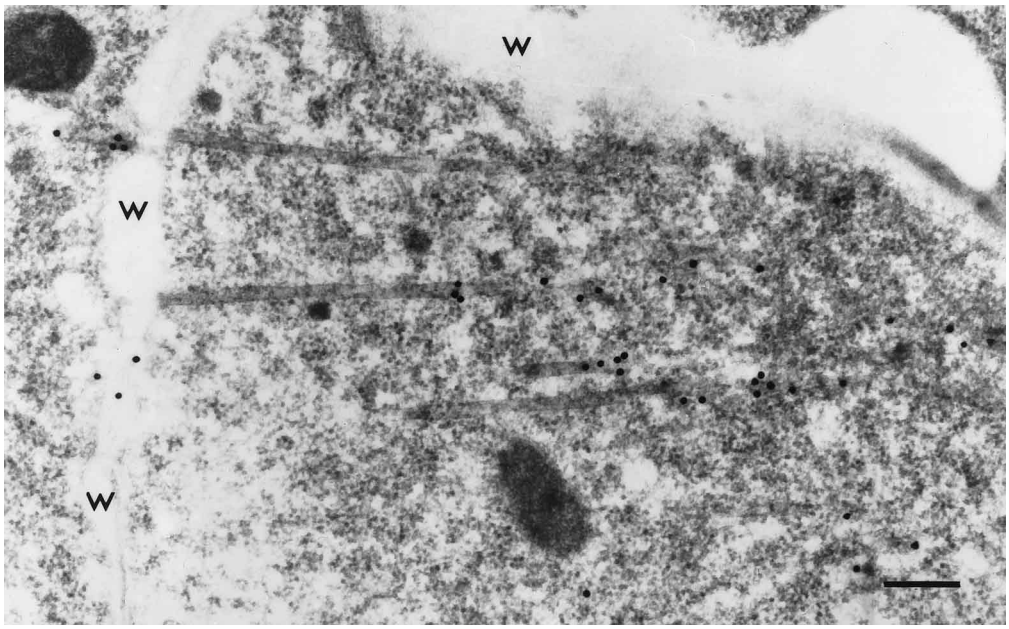


FIG. 2. Array of tubules in a procambial cell in an immature pumpkin leaf systemically infected with SqLCV. Tubules are arranged perpendicular to the cell wall (w). The section is labeled with antisera to BiP and protein A-gold. Scale bar, 200 nm.

eliminated. Additionally, virus-like particles were not seen within, or associated with, the tubules.

Tubules were somewhat variable in size: 90% were in the range of 30 to 50 nm in diameter, and the mean diameter was $36.8 \pm 1.2$ nm (standard error; $n = 36$). The longest measured tubule was 1.6 μm in length; however, since they passed into and out of the plane of section, some tubules were undoubtedly much longer. Tubules were usually separate from one another near the cell walls, but clustering of tubules was occasionally seen deeper in the cytoplasm (Fig. 2 and data not shown). In many sections, the tubules were closely associated with vacuoles, often curving around them (Fig. 3C), but the vacuoles in young procambial initials are so numerous that this association may be incidental.

**Antisera to both BL1 and BiP specifically stain the SqLCV tubules.** To investigate the nature and possible origins of these tubules, we performed immunogold labeling studies. Tubules were specifically labeled with anti-BL1 antisera (Fig. 3B to D and 4A). Some tubules were labeled for BL1 along their entire length (Fig. 3B and D and 4A); however, BL1 labeling was often pronounced near the visible ends of the tubules (Fig. 3C). This could be due to incomplete penetration of the antibody into the plastic such that only regions of the tubules that lie at the exposed surface of the sections, such as the cut ends, were subject to labeling by the antibody. Another possibility is that the antigenic sites are inside the tubule and are subject to antibody labeling only where the lumen is exposed by sectioning. Nevertheless, all of the tubules were of the same distinct type visually, and all of these tubules in a given section were specifically labeled with anti-BL1 antisera. Thus, there appeared to be only one population of SqLCV tubules. In addition, in serial thin sections, anti-BL1 antisera labeled tubules lying in the same area (not shown).

The tubules were not labeled by preimmune sera, nor were they labeled by antisera to BR1 (Fig. 4B and C), although the latter did label nuclei of procambial cells in regions where the tubules were seen. We have previously shown that anti-BR1 antisera label nuclei of phloem parenchyma cells in SqLCV-infected plants (11). Thus, BL1 labeling of the tubules was highly specific.

There are no structures in the cytosol of uninfected plants that correspond to the tubules reported here. We therefore considered whether the tubules might be derived from elements of the cytoskeleton or endomembrane system in developing phloem cells. The tubules described here are considerably larger than and distinct in appearance from microtubules, which are 24 nm in diameter. Unlike the TMV 30-kDa protein (36), BL1 does not appear to associate with tubulin in vitro (60a). However, the tubules do resemble the cortical ER when it is compressed in the cell plate during the formation of plasmodesmata (20, 39). Thus, to determine whether the BL1-containing tubules might be formed from modified ER, we performed immunogold labeling studies using antisera to binding protein (BiP), which itself specifically localizes to the lumen of the ER and is highly conserved among diverse species of animals and plants (1, 11, 14, 16, 58). The antisera used here react with BiP from several plant species (16). On immunoblots, this anti-BiP antisera specifically labeled only a single protein from pumpkin extracts (Fig. 5A). This protein was of the same molecular mass (75 kDa) as the BiP from maize, against which it was raised, and BiP from other plants (14).

Anti-BiP antisera labeled the tubules strongly and specifically (Fig. 2 and 3A). Tubules were not labeled by the BiP preimmune serum (not shown). Furthermore, antisera to BiP labeled these tubules in a pattern identical to that of anti-BL1 antisera, labeling tubules along their entire length (Fig. 2), but also heavily labeling tubules at their cut ends (Fig. 2 and 3A; compare to Fig. 3B to D and 4A). Moreover, as found for labeling with anti-BL1 antisera, all the tubules within a given section were labeled with the anti-BiP antisera. Thus, the BL1-associated tubules appear to be derived from the ER.

**BL1 cofractionates with BiP- and ER membrane-containing fractions from infected pumpkin.** To obtain independent evidence for the association of BL1 with ER-derived membranes, and thereby further link our immunogold studies with our earlier biochemical and genetic studies demonstrating the role

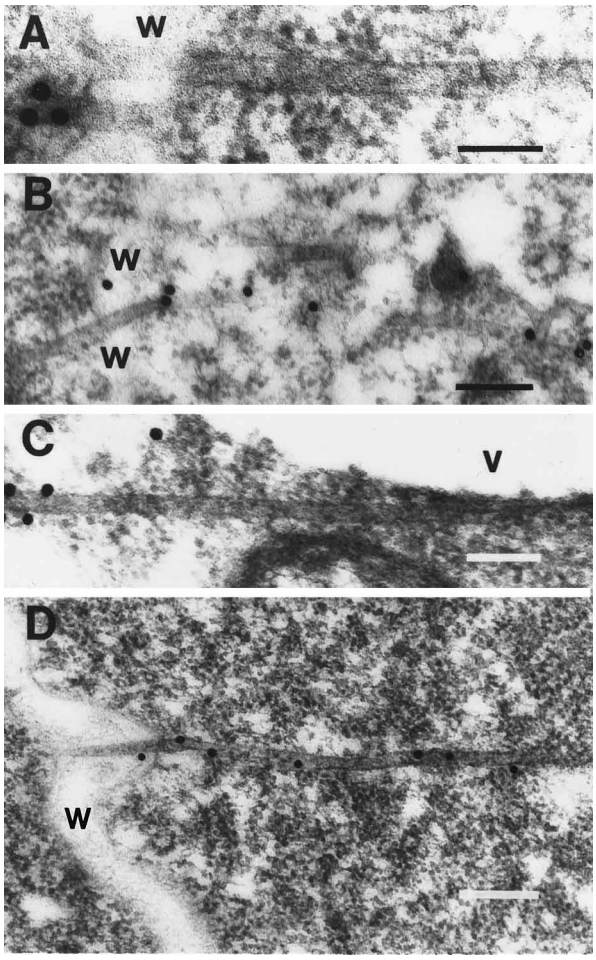


FIG. 3. Orientation of tubules in procambial cells. Sections were labeled with antisera as indicated below and protein A-gold. (A) Tubules crossing the cell wall (w), in a higher magnification view of the section shown in Fig. 2, labeled with anti-BiP antisera. The cut end of one tubule is labeled with three gold particles. Scale bar, 200 nm. (B) Tubules in the cytoplasm and crossing the cell wall (w), labeled with anti-BL1 antisera. Scale bar, 150 nm. (C) Tubule in close association with a vacuole (v), labeled with anti-BL1 antisera. Scale bar, 125 nm. (D) Tubule crossing a wall (w) that has been cut obliquely, labeled with anti-BL1 antisera. The tubule appears to narrow in the wall, probably due to its passing out of the plane of the section. Note, in addition to the gold particles along the length of the tubule in the cytoplasm, a gold particle over the portion of the tubule within the wall. Scale bar, 200 nm.

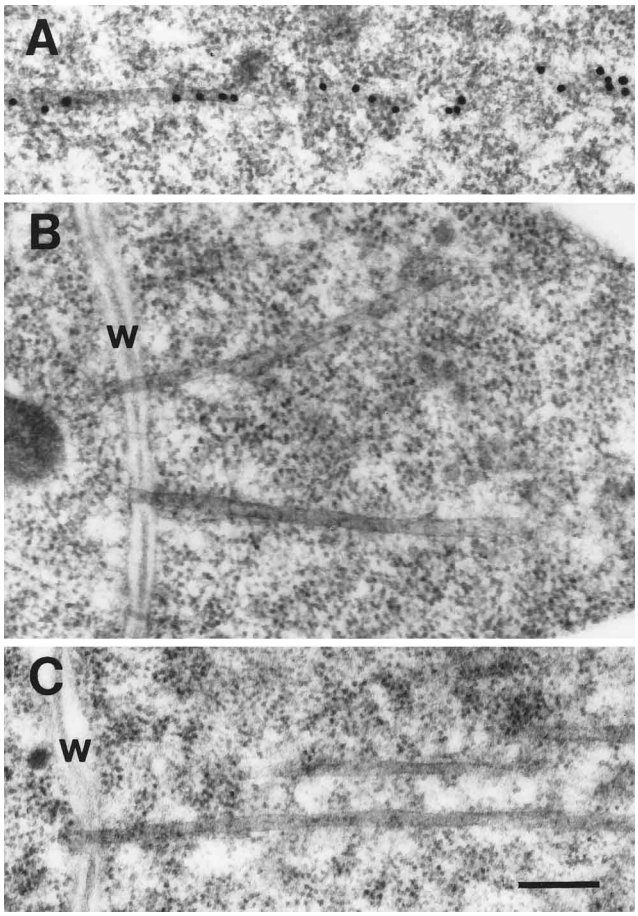


FIG. 4. Labeling of tubules with antisera to movement proteins and protein A-gold. (A) Anti-BL1 antisera; (B) anti-BR1 antisera; (C) preimmune serum from the generation of BL1 antibody. Scale bar, 200 nm.

of BL1 in virus movement (22, 41, 48), we prepared extracts from BL1-containing systemically infected pumpkin leaves and fractionated these by differential centrifugation and the aqueous two-phase partition method (28) to obtain plasma membrane-, ER-, and Golgi-containing fractions. Previous studies have shown BL1 to be associated with cell membrane-containing fractions, including specifically plasma membrane, from severely symptomatic systemically infected pumpkin leaves much older than those used here, and from leaves of transgenic plants (41).

The S1 supernatant was subjected to differential centrifugation to obtain a 5,200 $\times$ $g_{av}$ pellet (P2) and a 100,000 $\times$ $g_{av}$ pellet (P3) (see Materials and Methods). Based on assays for marker enzymes, 80% of the recovered Golgi membranes (Triton-stimulated IDPase activity) and 86% of the recovered plasma membranes (vanadate-sensitive $K^+$-$Mg^{2+}$-ATPase) fractionated to the P2 pellet, while 73% of the recovered ER membranes (antimycin A-insensitive NADH-dependent cytochrome *c* reductase activity) remained in the S2 supernatant and were recovered in the P3 pellet. Consistent with this finding, most of the BiP was also found in the ER membrane-containing P3 pellet as determined by immunoblotting (Fig. 5A).

Golgi, ER, and plasma membranes were further separated by the aqueous two-phase partition method. Based on the marker enzyme assays, 95% of the recovered Golgi membrane activity in the P2 pellet partitioned to the lower dextran phase and 64% of the recovered plasma membranes partitioned to the upper polyethylene glycol (PEG) phase. All of the recovered ER membrane activity (100%) from the P3 pellet partitioned to the lower dextran phase, and all of the BiP as detected by immunoblotting copartitioned with the ER membranes to this phase (Fig. 5A).

By immunoblotting, BL1 partitioned between the P2 and P3 fractions (Fig. 5B) and ~80% of BiP was found in the P3 fraction, which also contained the majority of the ER activity. All of the BL1 recovered in the P3 pellet coseparated with both the ER membrane activity and BiP to the lower phase in the aqueous two-phase partition assay (Fig. 5B). BL1 recovered in the P2 fraction, which contained both Golgi and plasma membranes, fractionated to the upper PEG phase along with the plasma membrane in the aqueous two-phase partition system (Fig. 5B). This result is consistent with our previous studies

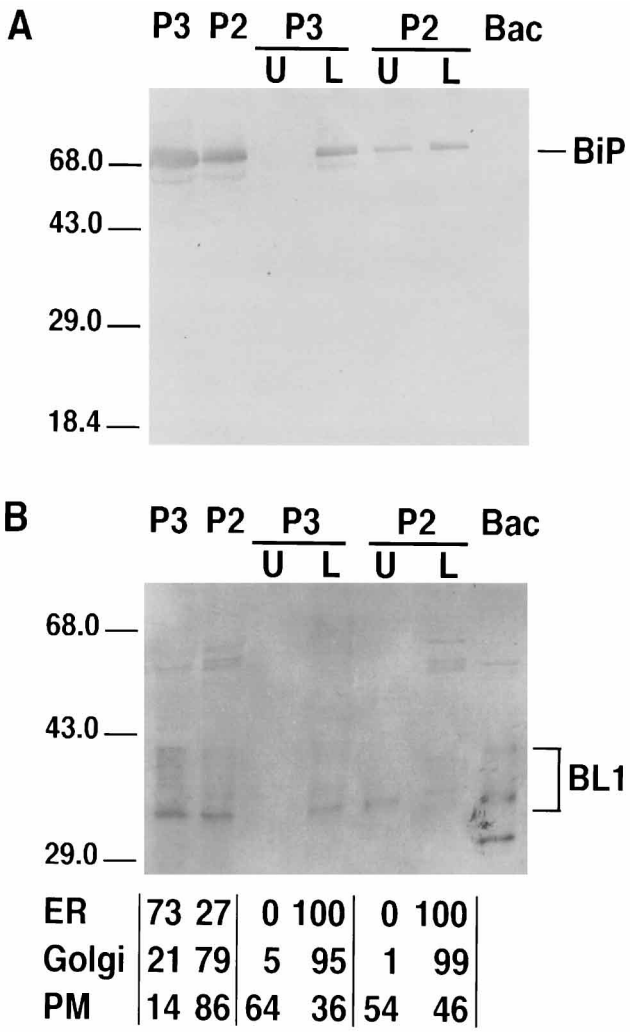


FIG. 5. Cofractionation of BL1 with BiP- and ER-containing membranes from SqLCV systemically infected pumpkin leaves. Aliquots of the 5,200 × $g_{av}$ (P2) or 100,000 × $g_{av}$ (P3) pellet, or of the upper PEG (U) or lower dextran (L) partitioned phases from the P2 or P3 pellet, from infected plants were immunoblotted in duplicate, and each blot was incubated with either anti-BiP (A) or anti-BL1 (B) antisera. The activities of marker enzymes for ER, Golgi, and plasma membranes (PM) in each fraction, expressed as the percentage of total recovered activity for each, are listed below the gel. Bac, extract from BL1-expressing recombinant baculovirus-infected *Spodoptera frugiperda* Sf9 cells. The ~29-kDa band is a breakdown product sometimes detected in BL1-containing preparations. Higher molecular mass bands in panel B are also detected by preimmune sera (38). See text for details. Molecular masses are indicated in kilodaltons.

(41). Thus, as determined by assaying for both BiP and marker enzyme activities, about two-thirds of BL1 from the young systemically infected leaves used here cofractionated with ER and/or ER-derived membranes, confirming and extending our immunogold labeling studies. In addition, the remaining BL1 was found to cofractionate with plasma membranes from these leaves. The amount of total BL1 in the plasma membrane-containing fraction appeared to increase at later stages of severe symptom development (data not shown) when total BL1 levels were found to decrease (Fig. 1). This finding is consistent with our previous studies demonstrating that the majority of BL1 coseparates with plasma membrane-containing fractions from systemically infected leaves that display severe disease symptoms and are more mature than those used in the studies reported here (41).

## DISCUSSION

Do all plant viruses use the same mechanisms and pathways to move their genomes? Based on recent studies, it has been suggested that this may be the case, with viral movement proteins acting both as chaperones to target the viral genome to plasmodesmata and as modulators of channel size to increase the size exclusion limits of plasmodesmata (15, 21, 34, 60). These and other studies (24, 32, 46, 56, 61) have focused on MP function in mesophyll cells, paying less attention to transport in the phloem, which is required for all plant viruses to move long distances and spread systemically in the host. In addition, arguments for a common mechanism and pathways for virus movement have not accounted for tubular structures found in mesophyll cells infected with several diverse plant viruses (24, 32, 46, 56, 61). The phloem limitation of SqLCV has provided an opportunity to study movement of virus within the phloem and to test some assumptions concerning MP function.

**Relationship of tubules to SqLCV movement.** The evidence indicates that the tubules described here function in the movement of SqLCV. The tubules were seen only in pumpkin plants inoculated with wild-type SqLCV, not in uninfected plants or in plants infected with the missense mutants $BL1^{R96A}$ and $BL1^{W208A}$, both of which produce nonfunctional BL1 and are defective in movement and null for infectivity (22, 47, 48). Consistent with the phloem limitation of SqLCV infection, tubules were found only in procambial cells, not in immature or mature mesophyll. In addition, the tubules clearly crossed the walls of procambial cells, suggestive of a role in cell-to-cell movement.

Most importantly, the tubules were specifically labeled by anti-BL1 antisera. Genetic studies demonstrate that BL1 is essential for systemic infection by all bipartite geminiviruses, including SqLCV (5, 13, 22). Furthermore, BL1, when expressed in protoplasts, has the intrinsic properties of targeting to the cortical cytoplasm and cell periphery and acting as a cytoplasmic trap for the movement protein BR1 to also redirect it from the nucleus to the cell periphery (47, 48). *BL1* mutants that mistarget to the cytoplasm and/or cannot redirect BR1 to the cell periphery are all movement defective in plants (22, 48).

The presence of tubules further correlated with the kinetics of BL1 expression and symptom development and the association of BL1 with BiP- and ER membrane-containing fractions. As symptoms progressed and infected leaves matured, BL1 levels and the amount of BL1 associated with ER membrane-containing fractions declined while levels of BL1 associated with plasma membrane-containing fractions increased (Fig. 1 and 5 and reference 41). Tubules were present at the time of maximal BL1 expression but were not detected in more mature and highly symptomatic leaves. This pattern of expression correlates with the timing of virus movement as visualized by the green fluorescent protein: when green fluorescent protein is substituted for the coat protein (AR1) of SqLCV, the virus is seen to move within systemically infected pumpkin leaves prior to the development of severe disease symptoms, and movement essentially ceases in mature, highly symptomatic leaves (28a).

**Comparison of SqLCV-associated tubules to those produced by other viruses.** Several features of the tubules reported here appear to distinguish them from tubules reported for other plant viruses (24, 32, 46, 57, 61). They are narrower (average

diameter, ~37 nm) than those induced by como-, tospo-, and caulimoviruses (~40 to 50 nm) or nepoviruses (~80 nm). No virus-like particles were associated with the tubules. This result correlates well with the finding that SqLCV lacking coat protein retains high levels of infectivity for cucurbits (22). In contrast to this, where virus-like particles associated with tubular structures have been well documented, the coat protein is essential for systemic infection (24, 32, 46, 57, 61). The BL1-associated tubules reported here can be seen to cross the walls of procambial cells and project into the cytoplasm on either side, whereas the tubules described for other plant viruses appear to project into the cytoplasm from only one side of the wall of mesophyll cells (24, 32, 46, 57, 61). Finally, in contrast to the MPs of CPMV (comovirus), tomato spotted wilt virus (tospovirus), and cauliflower mosaic virus (caulimovirus), which when transiently expressed in protoplasts induce the formation of long tubular projections (44, 46, 51, 56), neither SqLCV infection nor BL1 expression induces such structures in protoplasts (47, 48).

It may be that SqLCV tubules have unique features because they are made in a specialized tissue cell type and/or because they do not transport virus particles, as do other virus-induced tubules. Viewed from the opposite perspective, the unique nature of the tubules may reflect a distinct origin and unique features of the mechanism of SqLCV movement associated with the phloem limitation of this virus.

Tubules of the comovirus type have been reported for an uncloned field isolate of the geminivirus Euphorbia mosaic virus (23), but they do not appear to be of the same type as the tubules described here. The Euphorbia mosaic virus-associated tubules were reported to have virus-like particles within them. Using the same fixation conditions under which we see the BL1-associated tubules, we found arrays of geminate particles in the nuclei of phloem cells in SqLCV systemically infected leaves (data not shown), a well-documented characteristic of geminivirus infections (18). Thus, if virus particles were associated with the SqLCV BL1 tubules, we would have detected them. The Euphorbia mosaic virus-associated tubules were seen only in mesophyll cells from primary inoculated leaves, not in systemically infected leaves, which raises the question of their relevance to virus movement (23). Euphorbia mosaic virus infection was not phloem limited and, uncharacteristic for geminivirus infections, virus-like particles were reported to be in the cytoplasm. No immunogold labeling studies were done to further identify the nature of the tubules or identify the virus-like particles as being Euphorbia mosaic virus particles. In view of these important differences, the relationship of the tubules reported by Kim and Lee (23) to those reported here and to virus movement is difficult to assess.

**Tubules and plasmodesmata.** If SqLCV tubules penetrate preexisting plasmodesmata, no structural evidence of this association remained in the micrographs obtained to date. This is also true of the published micrographs of tubules formed by tomato spotted wilt virus, CPMV, and cauliflower mosaic virus, for which a plasmodesmal association has been suggested (24, 32, 46, 57, 61). The protocols for tissue preparation used in our study were designed to preserve antigenicity and to stain the tissue lightly. Under these conditions, lipid is extracted and the membranous components of plasmodesmata are difficult to see. In contrast, the tubules are well preserved and easily visible. This not only distinguishes the BL1-associated tubules from plasmodesmata and unmodified ER but also indicates that the walls of the tubules may be largely proteinaceous. The large size of the BL1 tubules where they cross the wall is also inconsistent with the diameter of a plasmodesma. Thus, if a BL1 tubule breaches the cell wall by penetrating a plasmodesma, then it highly modifies it and displaces the desmotubule.

On the other hand, as the desmotubule of a plasmodesma is a modification of, and links, the ER in adjoining cells (3, 33), specific staining of the BL1 tubules for the conserved ER lumenal protein BiP (14, 16, 58) suggests involvement of either plasmodesmata or the signaling pathway leading to the creation of plasmodesmata in the formation of BL1 tubules. This association was independently demonstrated by our finding that BL1 cofractionated, both by differential centrifugation and by aqueous two-phase partitioning, with BiP- and ER membrane-containing fractions from young infected systemic leaves of pumpkin plants. One possibility is that BL1 recruits the ER of an infected cell to form channels through the wall in much the same way as cortical ER is recruited to form the desmotubule in a plasmodesma. Whether this recruitment occurs during formation of the cell wall during cytokinesis (20), or whether the wall is breached after it is laid down, either in conjunction with or independent of preexisting plasmodesmata, is not known and is the subject of our current studies.

While anti-BiP antisera heavily stained the tubules, they did not stain ER in the cytosol. This was not necessarily unexpected, as BiP is normally expressed at a low constitutive level but is induced in response to stress and/or alterations in protein processing or the assembly of oligomeric structures (25, 37, 64). The antisera which we used, which was raised against BiP from maize, stain the ER and protein bodies in maize endosperm mutants with highly induced levels of BiP, but not in thin sections of normal maize endosperm (64). It is likely that the situation here may be similar to that in abnormal protein body formation, with BL1 expression and the assembly of the tubules resulting in the induction of increased levels of BiP. That the anti-BiP antisera expressly recognized BiP was demonstrated on Western blots, where they specifically recognized a single ~75-kDa protein that cofractionated with ER membrane-containing fractions and appeared to be the homolog of the 75-kDa BiP found in maize and other plant species (11, 14, 64).

**Structural and temporal aspects of SqLCV movement.** BL1 and BR1 have been shown to interact with each other in a cooperative manner, with BR1 binding the viral ssDNA genome and BL1 providing directionality to virus movement (47–49). How these functions are coordinated with tubule assembly and integrated with tubule structure remains to be shown. How tubule formation is coordinated with the development of the phloem and the progression of disease symptoms, as suggested by our data, must also be addressed.

While it remains to be determined whether BL1 is incorporated into the wall of the tubule or is being transported by it, the unique appearance of the tubules and their stability following chemical fixation, which exceeds that of the normal endomembrane system, indicate that BL1 may be part of the tubule itself. That the tubules were not stained by antisera against BR1, although BR1 was detected in the nuclei of procambial cells where the tubules were seen (data not shown), suggests that BR1 is not a structural component of the tubule. This is consistent with a transient association of BR1 with the tubules, implicit in its role as a nuclear shuttle protein that complexes with the viral ssDNA genome to move it (42, 47, 48).

We propose that BL1-containing tubules serve as a conduit for the transport of BR1, and its associated viral ssDNA, from one cell to another. Together with our previous demonstration that BL1 alone is directly responsible for SqLCV pathogenic effects seen in infected plants (22, 41), our results suggest that BL1 functions early in infection of the leaf to ensure virus

movement into adjoining cells, with the further progression of disease symptoms being a secondary effect of this function of BL1. The presence of virus in the developing phloem would appear to provide an efficient mechanism for the virus to invade the infected leaf. It would further ensure that as the venation becomes functional during leaf growth and the leaf begins to export (54, 55), the viral genome would be present in functioning small veins and from these transported out of the leaf to continue the infectious cycle throughout the plant.

Another model for the action of BL1 has been put forward, based on microinjection studies of mature tobacco mesophyll cells (38). According to this model, BL1 encoded by bean dwarf mosaic virus (BDMV) behaves similarly to the TMV MP, increasing the size exclusion limits of plasmodesmata and rapidly moving itself cell to cell (38). Tubules were not reported in the BDMV studies, and the very rapid movement reported for fluorescently tagged BDMV BL1 would appear to be inconsistent with the formation of the extensive tubules that we report here. The fact that in these same studies microinjected BR1 did not enter the nucleus, in contrast to studies that demonstrate the presence of BR1 in nuclei of several different cell types and the importance of BR1 nuclear targeting for its in vivo function (42, 47, 48), suggests that there may be problems associated with the preparation of proteins and/or microinjection techniques used in the BDMV studies. Differences could also result from the different cell types studied—mature tobacco mesophyll cells in the BDMV studies and developing pumpkin phloem cells investigated here—as well as the stage of development of the cells, which is known to affect MP function (12, 61). It may also be that, despite the extremely high degree of sequence conservation among BL1 proteins encoded by different bipartite geminiviruses (40), each has adapted its function to the different cellular milieus encountered by phloem-restricted and mesophyll-replicating geminiviruses. The factors important in explaining these differences remain to be determined. Nevertheless, our findings do suggest a process for creating channels for virus movement in SqLCV-infected phloem cells that differs from that suggested by studies on TMV and red clover necrotic mosaic virus in mesophyll cells (15, 60, 63).

In the broader context, there is an emerging picture of viruses using components of the cell's cytoskeleton and endomembrane system to move their genomes. While the role of the cytoskeleton in the movement of viral genomes during virus penetration, assembly, and egress has long been documented for several animal viruses (4, 7, 43, 45, 52), only recently are comparable studies being done for plant viruses. Recent studies show the TMV MP to be associated with microtubules in both infected plants and tobacco protoplasts (19, 36). It is possible that similar cellular elements, such as the ER and microtubules, have been adapted by different viruses in ways best suited for the movement of each viral genome. Localization of BL1 and other MPs in serial sections and through developmental series, and the identification of cell proteins that interact with the different MPs, including BL1, will address these issues. Beyond its importance in SqLCV movement, further investigation of BL1 function should undoubtedly advance our understanding of the biogenesis of channels through plant cell walls.

## ACKNOWLEDGMENTS

We thank Rebecca Boston for providing the anti-BiP antibodies, Steve Micklasz and Amy Hamilton for assistance in preparing anti-BR1 and anti-BL1 antisera, Dan Bush for suggestions for isolating membrane-containing fractions, and M. V. Parthasarathy for advice on electron microscopy.

This work was supported by grants from the National Science Foundation (IBN-9419703) and U.S. Department of Agriculture Competitive Grants Program (94-37306-0351) to R.T. and by grants from the National Science Foundation (MCB-9417664) and the University of Illinois Research Board to S.G.L.

## REFERENCES

1. **Anderson, J. V., Q.-B. Li, D. W. Haskell, and C. L. Guy.** 1994. Structural organization of the spinach endoplasmic reticulum-luminal 70-kilodalton heat-shock cognate gene and expression of 70-kilodalton heat shock genes during cold acclimation. Plant Physiol. **104:**1359–1370.
2. **Atabekov, J. G., and Y. L. Dorokhov.** 1984. Plant virus-specific transport function and resistance of plants to viruses. Adv. Virus Res. **29:**313–363.
3. **Beebe, D. U., and R. Turgeon.** 1991. Current perspectives on plasmodesmata: structure and function. Physiol. Plant. **83:**194–199.
4. **Ben-Ze'ev, A., R. Abulafia, and Y. Aloni.** 1982. SV40 virions and viral RNA metabolism are associated with cell substructures. EMBO J. **1:**1225–1231.
5. **Brough, C. L., R. J. Hayes, A. J. Morgan, R. H. Coutts, and K. W. Buck.** 1988. Effects of mutagenesis *in vitro* on the ability of cloned tomato golden mosaic virus DNA to infect *Nicotiana benthamiana* plants. J. Gen. Virol. **69:**503–514.
6. **Bush, D. R.** 1989. Proton-coupled sucrose transport in plasmalemma vesicles isolated from sugar beet leaves. Plant Physiol. **89:**1318–1323.
7. **Chatterjee, P., M. Cervera, and S. Penman.** 1984. Formation of vesicular stomatitis virus nucleocapsid cytoskeleton framework-bound N protein: possible model for structure assembly. Mol. Cell. Biol. **4:**2231–2234.
8. **Citovsky, V., D. Knorr, G. Schuster, and P. Zambryski.** 1990. The P30 movement protein of tobacco mosaic virus is a single-stranded nucleic acid binding protein. Cell **60:**637–647.
9. **Citovsky, V., M. L. Wong, A. L. Shaw, B. V. Venkataram Prasad, and P. Zambryski.** 1992. Visualization and characterization of tobacco mosaic virus movement protein binding to single-stranded nucleic acids. Plant Cell **4:**397–411.
10. **Citovsky, V., and P. Zambryski.** 1993. Transport of nucleic acids through membrane channels: snaking through small holes. Annu. Rev. Microbiol. **47:**167–197.
11. **Denecke, J., M. H. S. Goldman, J. Demolder, J. Seurinck, and J. Botterman.** 1991. The tobacco luminal binding protein is encoded by a multigene family. Plant Cell **3:**1025–1035.
12. **Epel, B. L.** 1994. Plasmodesmata: composition, structure and trafficking. Plant Mol. Biol. **26:**1343–1356.
13. **Etessami, P., R. Callis, S. Ellwood, and J. Stanley.** 1988. Delimitation of the essential genes of the cassava latent virus DNA 2. Nucleic Acids Res. **16:** 4811–4829.
14. **Fontes, E. B. P., B. B. Shank, R. L. Wrobel, S. P. Moose, G. R. OBrian, E. T. Wurtzel, and R. S. Boston.** 1991. Characterization of an immunoglobulin binding protein homolog in the Maize *floury-2* endosperm mutant. Plant Cell **3:**483–496.
15. **Fujiwara, T., D. Giesman-Cookmeyer, B. Ding, S. A. Lommel, and W. J. Lucas.** 1993. Cell-to-cell trafficking of macromolecules through plasmodesmata potentiated by the red clover necrotic virus movement protein. Plant Cell **5:**1783–1794.
16. **Gilikin, J. W., E. P. B. Fontes, and R. S. Boston.** 1995. Protein-protein interactions within the endoplasmic reticulum. Methods Cell Biol. **50:**309–323.
17. **Goldbach, R., J. Wellink, J. Verver, A. van Kammen, D. Kasteel, and J. van Lent.** 1994. Adaptation of positive-strand RNA viruses to plants. Arch. Virol. Suppl. **9:**87–97.
18. **Goodman, R. M.** 1981. Geminiviruses, p. 879–910. *In* E. Kurstak (ed.), Handbook of plant virus infection and comparative diagnosis. Elsevier/North Holland Biomedical Press, New York, N.Y.
19. **Heinlein, M., B. L. Epel, H. S. Padgett, and R. N. Beachy.** 1996. Interaction of tobamovirus movement proteins with the plant cytoskeleton. Science **270:**1983–1985.
20. **Hepler, P. K.** 1982. Endoplasmic reticulum in the formation of the cell plate and plasmodesmata. Protoplasma **111:**121–133.
21. **Hull, R.** 1991. The movement of viruses within plants. Semin. Virol. **2:**89–95.
22. **Ingham, D. J., E. Pascal, and S. G. Lazarowitz.** 1995. Both geminivirus movement proteins define viral host range, but only BL1 determines viral pathogenicity. Virology **207:**191–204.
23. **Kim, K.-S., and K.-W. Lee.** 1992. Geminivirus-induced macrotubules and their suggested role in cell-to-cell movement. Phytopathology **82:**664–669.
24. **Kormelink, R., M. Storms, J. van Lent, D. Petters, and R. Goldbach.** 1994. Expression and subcellular localization of the $NS_M$ protein of tomato spotted wilt virus (TSWV), a putative viral movement protein. Virology **200:**56–65.
25. **Kozutsumi, Y., M. Segal, K. Normington, M. J. Gething, and J. Sambrook.** 1988. The presence of malfolded proteins in the endoplasmic reticulum signals the induction of glucose-regulated proteins. Nature **332:**462–464.
26. **Laemmli, U. K.** 1970. Cleavage of structural proteins during the assembly of the head of bacteriophage T4. Nature **227:**680–685.
27. **Lapidot, M., R. Gafny, B. Ding, S. Wolf, W. J. Lucas, and R. N. Beachy.** 1993. A dysfunctional movement protein of tobacco mosaic virus that partially

modifies the plasmodesmata and limits virus spread in transgenic plants. Plant J. **4:**959–970.
28. **Larsson, C.** 1985. Plasma membranes, p. 85–104. *In* H. F. Linskens and J. F. Jackson (ed.), Modern methods of plant analysis, vol. 1. Springer-Verlag, Berlin, Germany.
28a. **Laukaitis, C. M., and S. G. Lazarowitz.** Unpublished results.
29. **Lazarowitz, S. G.** 1992. Geminiviruses: genome structure and gene function. Crit. Rev. Plant Sci. **11:**327–349.
30. **Lazarowitz, S. G.** 1991. Molecular characterization of two bipartite geminiviruses causing squash leaf curl disease: role of viral replication and movement functions in determining host range. Virology **180:**70–80.
31. **Lazarowitz, S. G., and I. B. Lazdins.** 1991. Infectivity and complete nucleotide sequence of the cloned genomic components of a bipartite squash leaf curl geminivirus with a broad host range phenotype. Virology **180:**58–69.
32. **Linstead, P. J., G. J. Hills, K. A. Plaskitt, I. G. Wilson, C. L. Harker, and A. J. Maule.** 1988. The subcellular localization of the gene 1 product of cauliflower mosaic virus is consistent with a function associated with virus spread. J. Gen. Virol. **69:**1809–1818.
33. **Lucas, W. J., B. Ding, and C. van der Schoot.** 1993. Plasmodesmata and the supracellular nature of plants. New Phytol. **125:**435–476.
34. **Lucas, W. J., and R. L. Gilbertson.** 1994. Plasmodesmata in relation to viral movement within leaf tissues. Annu. Rev. Phytopathol. **32:**387–411.
35. **Malyshenko, S. I., O. A. Kondakova, J. V. Nazarova, I. B. Kaplan, M. E. Taliansky, and J. G. Atabekov.** 1993. Reduction of tobacco mosaic virus accumulation in transgenic plants producing non-functional viral transport proteins. J. Gen. Virol. **74:**1149–1156.
36. **McLean, B. G., J. Zupan, and P. C. Zambryski.** 1996. Tobacco mosaic virus movement protein associates with the cytoskeleton in tobacco cells. Plant Cell. **7:**2101–2114.
37. **McMillan, D. R., M. J. Gething, and J. Sambrook.** 1994. The cellular response to unfolded proteins: intercompartmental signaling. Curr. Opin. Biotechnol. **5:**540–545.
38. **Noueiry, A. O., W. J. Lucas, and R. L. Gilbertson.** 1994. Two proteins of a plant DNA virus coordinate nuclear and plasmodesmatal transport. Cell **76:**925–932.
39. **Overall, R. L., J. Wolf, and B. E. S. Gunning.** 1982. Intercellular communication in *Azolla* roots. I. Ultrastructure of plasmodesmata. Protoplasma **111:**134–150.
40. **Padidam, M., R. N. Beachy, and C. M. Fauquet.** 1995. Classification and identification of geminiviruses using sequence comparisons. J. Gen. Virol. **76:**249–263.
41. **Pascal, E., P. E. Goodlove, L. C. Wu, and S. G. Lazarowitz.** 1993. Transgenic tobacco plants expressing the geminivirus BL1 protein exhibit symptoms of viral disease. Plant Cell **5:**795–807.
42. **Pascal, E., A. A. Sanderfoot, B. M. Ward, R. Medville, R. Turgeon, and S. G. Lazarowitz.** 1994. The geminivirus BR1 movement protein binds single-stranded DNA and localizes to the cell nucleus. Plant Cell **6:**995–1006.
43. **Penfold, M. E., P. Armati, and A. L. Cunningham.** 1994. Axonal transport of herpes simplex virions to epidermal cells: evidence for a specialized mode of virus transport and assembly. Proc. Natl. Acad. Sci. USA **91:**6529–6533.
44. **Perbal, M.-C., C. L. Thomas, and A. J. Maule.** 1993. Cauliflower mosaic virus gene I product (P1) forms tubular structures which extend from the surface of infected protoplasts. Virology **195:**281–285.
45. **Quinlan, M. P., and D. M. Knipe.** 1983. Nuclear localization of herpes viral proteins: potential role for the cellular framework. Mol. Cell. Biol. **3:**315–324.
46. **Ritzenthaler, C., A.-C. Schmit, P. Michler, C. Stussi-Garaud, and L. Pinck.** 1995. Grapevine fanleaf nepoviruse P38 putative movement protein is located on tubules *in vivo*. MPMI **8:**379–387.
47. **Sanderfoot, A. A., D. J. Ingham, and S. G. Lazarowitz.** 1996. A viral movement protein as a nuclear shuttle: the geminivirus BR1 movement protein contains domains essential for interaction with BL1 and nuclear localization. Plant Physiol. **110:**23–33.
48. **Sanderfoot, A. A., and S. G. Lazarowitz.** 1995. Cooperation in viral movement: the geminivirus BL1 movement protein interacts with BR1 and redirects it from the nucleus to the cell periphery. Plant Cell **7:**1185–1194.
49. **Sanderfoot, A. A., and S. G. Lazarowitz.** 1996. Getting it together in plant virus movement: cooperative interactions between bipartite geminivirus movement proteins. Trends Cell Biol. **6:**353–358.
50. **Stanley, J.** 1985. The molecular biology of geminiviruses. Adv. Virus Res. **30:**139–177.
51. **Storms, M. M. H., R. Kormelink, D. Peters, J. W. M. Van Lent, and R. W. Goldbach.** 1995. The nonstructural NSm protein of tomato spotted wilt virus induces tubular structures in plant and insect cells. Virology **214:**485–493.
52. **Topp, K. S., L. B. Meade, and J. H. La La Vail.** 1994. Microtubule polarity in the peripheral processes of trigeminal ganglion cells: relevance for the retrograde transport of herpes simplex virus. J. Neurosci. **14:**318–325.
53. **Turgeon, R.** 1989. The sink-source transition in leaves. Annu. Rev. Plant Physiol. Plant Mol. Biol. **40:**119–138.
54. **Turgeon, R., and P. K. Hepler.** 1989. Symplastic continuity between mesophyll and companion cells in minor veins of mature *Cucurbita pepo* L. leaves. Planta **179:**24–31.
55. **Turgeon, R., and J. A. Webb.** 1976. Leaf development and phloem transport in *Cucurbita pepo*: maturation of the minor veins. Planta **129:**265–269.
56. **van Lent, J., M. Storms, F. van der Meer, J. Wellink, and R. Goldbach.** 1991. Tubular structures involved in movement of cowpea mosaic virus are also formed in infected cowpea protoplasts. J. Gen. Virol. **72:**2615–2623.
57. **van Lent, J., J. Wellink, and R. Goldbach.** 1990. Evidence for the involvement of the 58K and 48K proteins in the intercellular movement of cowpea mosaic virus. J. Gen. Virol. **71:**219–223.
58. **Vitale, A., A. Ceriotti, and J. Denecke.** 1993. The role of the endoplasmic reticulum in protein synthesis, modification and intracellular transport. J. Exp. Bot. **44:**1417–1444.
59. **Volk, G. M., R. Turgeon, and D. U. Beebe.** 1996. Secondary plasmodesmata formation in the minor vein phloem of *Cucumis melo L.* and *Cucurbita pepo L.* Planta **199:**425–432.
60. **Waigmann, E., W. J. Lucas, V. Citovsky, and P. Zambryski.** 1994. Direct functional assay for tobacco mosaic virus cell-to-cell movement protein and identification of a domain involved in increasing plasmodesmal permeability. Proc. Natl. Acad. Sci. USA **91:**1433–1437.
60a. **Ward, B. M., and S. G. Lazarowitz.** Unpublished results.
61. **Weiczorek, A., and H. Sanfacon.** 1993. Characterization and subcellular localization of tomato ringspot nepovirus putative movement protein. Virology **194:**734–742.
62. **Wellink, J., J. W. M. van Lent, J. Verver, T. Sijen, R. W. Goldbach, and A. van Kammen.** 1993. The cowpea mosaic virus M RNA-encoded 48-kilodalton protein is responsible for induction of tubular structures in protoplasts. J. Virol. **67:**3660–3664.
63. **Wolf, S., C. M. Deom, R. N. Beachy, and W. J. Lucas.** 1989. Movement protein of tobacco mosaic virus modifies plasmodesmatal size exclusion limit. Science **246:**377–379.
64. **Zhang, F., and R. S. Boston.** 1992. Increases in binding protein (BiP) accompany changes in protein body morphology in three high-lysine mutants of maize. Protoplasma **171:**142–152.